

Silver Nanoparticles (Ag NPs) Prepared By Laser Ablation In Ethanol

¹Duaa Jabbar Hussein , ²Muneer H. Jadaa Alzubaidy , ³Ahmed N. Abd

^{1,2}College of science, Wasit University, Wasit, Iraq

³Physics Department, Science Faculty, University of Al- Mustansiriyah, Baghdad, Iraq
Corresponding author. E-mail: ahmed_naji_abd@yahoo.com

Abstract—The effect of laser fluence on structural, morphological, optical, and electrical properties of Silver nanoparticles AgNPs prepared by irradiating a silver target, immersed in ethanol, with Nd:YAG laser pulses at laser fluence in the range of 1.32J/cm² has been studied. X-ray diffraction XRD measurements disclosed that the Ag NPs were of F.C.C crystal structure. AFM investigation revealed that the synthesized Ag NPs particles are spherical and have an average particle size in the range of (40-50 nm). The optical energy gap of Silver nanoparticles prepared has been determined from optical properties and found to be in the range of 1.95 Optical constants of Ag NPs were determined from transmittance and reflectance spectra.

Keywords—Silver , XRD, AFM, Laser ablation, optical properties

1. Introduction

In recent years, there has been a great interest in the preparation and application of the silver

and gold nanoparticles. Under the short laser pulse irradiation in the spectral range of the surface plasmon resonance, metal nanoparticles such as silver or gold nanoparticles are excited to upper electronic states by multiphoton absorption. Through rapid relaxation to their ground state, the absorption photon energy can be converted into thermal energy. Their temperature rises very quickly to reach thresholds for nonlinear effects such as optical plasma, micro bubble formation, acoustic and shock wave generation and particle fragmentation with fragments of high kinetic energy. The laser induced explosion of absorbing nanoparticles contributes a potential role for selective damage to cancer cells, bacteria, viruses and DNA.[1] Several methods to prepare metallic nanoparticles suspended in liquid have been developed [2, 3]. The wet preparation methods range from the synthesis by chemical reduction in solution, laser irradiation of the metallic salt solution to laser ablation of metal plate. The most interest is to produce stable nanoparticles of a controlled size and well-defined distribution. The stability, the size distribution and the abundance of the nanoparticles depend critically on the properties and concentration of the surfactant employed.

2. Results and discussion

2.1 XRD investigation

The XRD diffraction patterns of synthesized Ag nanoparticles film ablated in methanol and deposited on glass. The XRD patterns of Ag contain ten main peaks at diffraction angles : 38.12, 44.26, 64.44 and 77.4 corresponding to (111), (200), (220) and (311) planes respectively also. This result agrees well with that presented in references, [4]. All the diffraction peaks are indexed to FCC structure and there is no trace of hexagonal face which matches well the standard peaks (ASTM: Ag, no: 00-004-0783). The average crystallite size ($D=50$ nm) for a known X-ray wavelength λ at a diffraction angle θ of Ag nanoparticles is calculated by using **Scherrer** formula, the peak widths of a strong diffraction plane were calculated and listed in Table (1), the strong and narrow peaks may be ascribed to the preferential growth along (111) plane of Ag crystallites. The strain (η) and dislocation density (δ) were calculated and listed in Table (1). (η and δ) of Ag nanoparticles films were ablated in methanol at varies from $(7.2-6.42) \times 10^{-4}$ lines⁻². m⁻⁴. and $(3,5-4.3) \times 10^{14}$ lines . m⁻² respectively.

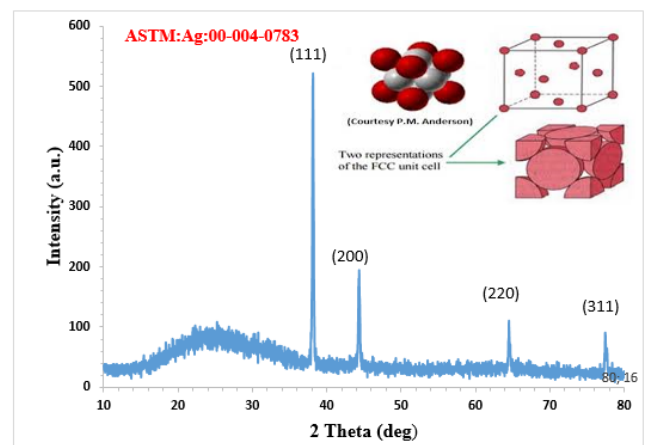


Figure (1) : XRD spectra of Ag thin film

Table (1) Summary of XRD characterization for Ag nanoparticles ablation in ethanol and deposited on a glass substrate.

2 Theta (deg)	FWHM (deg)	D (nm)	$\sigma \times 10^{14}$ lines.m ⁻²	Strain $\times 10^{-4}$ lines ⁻² .m ⁻⁴
38.11	0.175	47.789 59	4.3785802 81	7.2505323 97
44.3	0.21	40.650 86	6.0514659 04	8.5238055 6
64.46	0.17	55.038 27	3.3011896 88	6.2956196 01
77.4	0.19	53.428 65	3.5030926 75	6.4852847 94

2.2 Atomic force microscopy (AFM)

The 3D AFM images and granularity accumulation distribution chart of Ag NPs synthesized. The average grain size of doped and undoped synthesized Ag films is measured from AFM analysis using software and is found to be around 66.85 nm depending on preparation conditions.

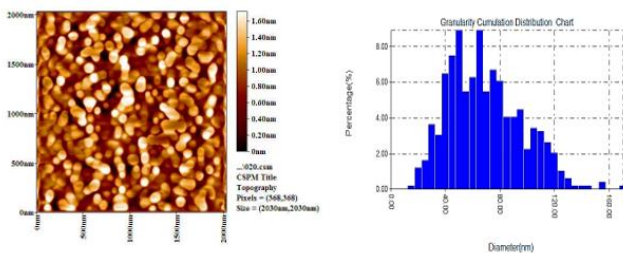


Fig.(2): 3D AFM image of and Granularity accumulation distribution chart of Ag nanoparticles ablation in ethanol.

The surface morphology of the undoped Ag thin films obtained from the AFM analysis as shown in the figure above. It is obvious that surface is very smooth. The average roughness of the film surface 0.382 nm.

Table (2): The grain size, roughness average and Root mean square for Ag NPs.

Sample	Average Grain size (nm)	Roughness average (nm)	RMS (nm)
Ag Thin film	66.85	0.311	0.382

2.3. Optical properties

Figure 3 shows the optical transmittance for Ag nanoparticles ablated in methanol by laser and deposited on glass substrate as a function the wavelength at range (300-900) nm. The figure have three region, the first one in UV range has a maximum value 78% of transmittance, exactly at 322 nm, also, the second region from the range (322-420) nm, in this region we, can see that decrease the transmittance to (52%) at the wavelength (420)nm and the last region above (420-900)nm, slowly increase in transmittance.

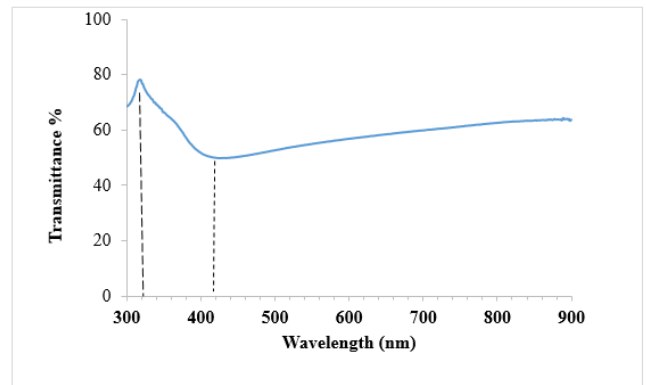


Fig. (3): Optical transmittance for Ag thin film deposited on a glass substrate as a function of wavelength.

The absorption characteristics can consider a useful tool to analyze nanomaterials. It is clearly seen that the absorption is decreasing sharply below ~400nm. It is observed that there are remarkable variations in absorption spectra in the range from 400nm to 500nm due to quantum size effect, which can be ascribed to the formation of Ag nanoparticles. This result agrees well with ref. [5-7]. Figure 4-4 shows the optical absorbance for Ag thin film deposited on a glass substrate as a function the wavelength at the range (300-900) nm. The figure has three regions, the first one in UV range has a maximum value (0.152 %) of absorbance, exactly at 318 nm, the second region at the range (318-478) nm, in this region we can see that increase the absorbance to (0.528 %) at wavelength (440 nm) and the last region above (440-900) nm, slowly decrease in absorbance.

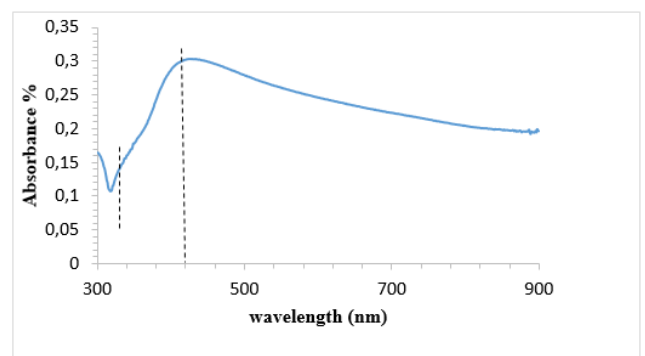


Fig. (4): Optical absorbance for Ag thin film deposited on a glass substrate as a function of wavelength.

The reflectance of Ag nanoparticles reflectance decreases with wavelength increase up to 400 nm, that the reflectance tends to saturate only, for Ag NPs prepared by 400 mJ laser energy is given in figure (5). Also the figure shows an increase in optical reflectance in colloidal nanoparticles Ag dissolved in methanol and it exhibits a strong red shift in its optical spectra [8-9].

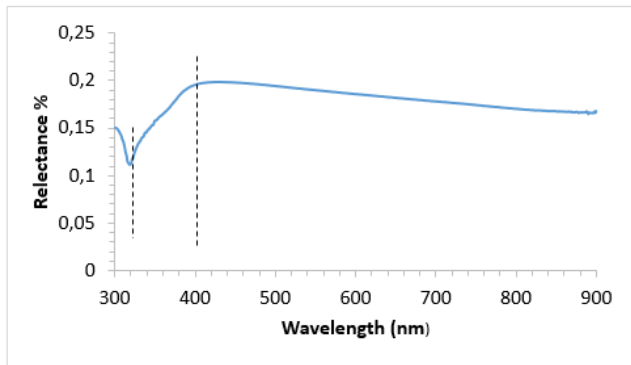


Fig. (5): Optical reflectance for Ag thin film deposited on a glass substrate as a function of wavelength.

Figure 6 shows the refractive index for the Ag thin film deposited on a glass substrate as a function the wavelength at the range (300-900) nm. The figure have three regions, the first one in UV range has a maximum value (0.15 %) of refractive index , exactly at (318 nm), the second region from range (318-430) nm, in this range we can see that increase the refractive index to (1.6) at wavelength (420 nm) and the last region above (420-900) nm, slowly decrease in refractive index.

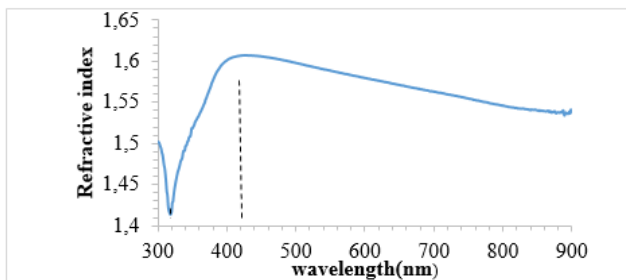


Fig. (6): The refractive index for the Ag thin film as a function of wavelength.

The energy band gap of Ag is estimated by plotting the square of $(\alpha h\nu)$ versus $(h\nu)$. The energy band gap (E_g) values depend on the film crystal structure, the arrangement and distribution of atoms in the crystal lattice. The optical band gap of 1.95 eV was estimated for pure Ag film. The values of the optical band gap of Ag NPs depending on laser fluence. Increasing the band gap with laser fluence is due to formation of nano-sized Ag particles and this result is supported by AFM.

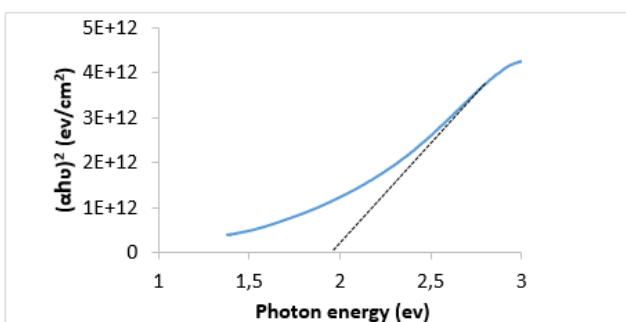


Fig.(7) $(\alpha h\nu)^2$ versus photon energy gap of Ag colloidal dissolved in ethanol .

Figure (8) shows the variation of real and imaginary part of the dielectric constant (ϵ_r and ϵ_i) respectively as a function of wavelength . It is found that ϵ_r decreases with increasing the wavelength , in another word decreasing the photon energy , but ϵ_i increased with increasing the photon energy ,also, the behavior of ϵ_r is similar reasons mentioned previously in the refractive index, while ϵ_i depended of extinction coefficient.

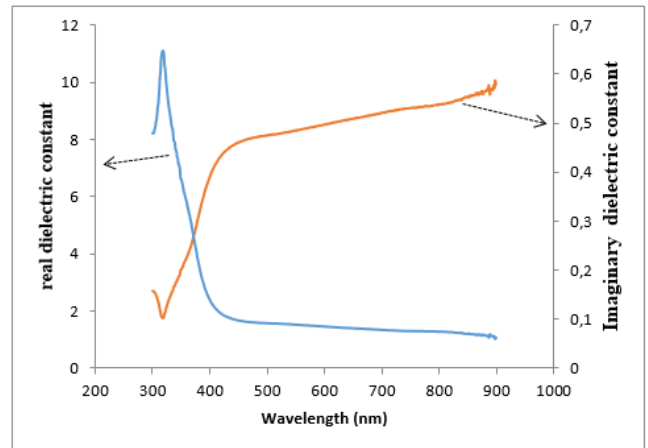


Figure (8): Imaginary part of dielectric constant as a function of wavelength for Ag thin film.

3. Conclusion

The reported study demonstrates the effect of solution type of structural, optical and morphological properties of Ag nanoparticles synthesised by laser ablation. To the best of our knowledge, the production of Ag nanoparticles in ethanol by laser ablation is reported for the first time. The produced nanoparticles were polycrystalline in nature with FCC phase. The optical properties data revealed that the direct optical band gap of Silver ablated in ethanol was 1.95 eV .

References

- [1] Renat R Letfullin, Charles Joenathan, Thomas F George, Vladimir P Zharov, *anomedicine*, 1(4) (2006) 473.
- [2] Fumitaka Mafune, Jun-ya kohno Yoshihiro Takeda, Tamotsu Kondow, *Journal of Physical Chemistry B*, Vol. 104 No35 (2000) 8333.
- [3] J.P.Abid, A.W.Wark P. F. Brevet, H.Girault, *J. Phys. Chem. B* 33 (2002) 792.
- [4] S.A. Mahmoud, A. Ashour, E.A. Badawi, Processing parameters and transport properties of vacuum evaporated CdSe thin films. *Appl. Surf. Sci.* 253, 2969–2972 (2006)
- [5] C. Petit, P. Lixon.P, M.P. Pileni, *Journal of Physical Chemistry*, 97 (1993) 12974.
- [6] U. Kreibig, M. Vollmer, *Optical properties of metal clusters*, Springer, Berlin, 1995.
- [7]. K.D. Patel, M.S. Jani, V.M. Pathak, R. Srivastava, Deposition of CdSe thin films by thermal

evaporation and their structural and optical properties. Chalcogenide Lett. 6(6), 279–286 (2009)

[8]. D. Patidar, K.S. Rathore, N.S. Saxena, K. Sharma, T.P. Sharma, Energy band gap and conductivity measurement of CdSe thin films. Chalcogenide Lett. 5(2), 21–25 (2008)

[9] O. Toma, S. Iftimie, C. Besleaga, T.L. Mitran, V. Gghenescu, O.Porumb, A. Toderas, M. Radu, L. Ion, S. Antohe, New investigations on cadmium sulfide thin films for photovoltaic applications. Chalcogenide Lett. 8(12), 747–756 (2011)